J. Inst. Eng. India Ser. C (April–June 2013) 94(2):123–133
DOI 10.1007/s40032-013-0068-y

ORIGINAL CONTRIBUTION

Conjugate Convection with Surface Radiation from a Square-Shaped Electronic Device with Multiple Identical Discrete Heat Sources

A. P. Shah · Y. M. Krishna · C. G. Rao

Received: 16 January 2013 / Accepted: 17 April 2013 / Published online: 2 June 2013

Abstract Numerical simulation studies on combined conduction–convection–radiation from a square-shaped electronic device with multiple identical flush-mounted discrete heat sources have been performed and the prominent results are reported here. The problem geometry comprises a square shaped slab with four symmetrically located flush mounted identical discrete heat sources. The heat generated in the heat sources gets conducted through the slab and subsequently gets dissipated from its boundaries by the combined modes of convection and radiation. Air, a radiatively transparent medium is considered to be the cooling agent. The governing equations for temperature distribution in the entire computational domain are obtained by appropriate energy balance between the heat generated, conducted, convected and radiated. The resulting partial differential equations are solved using finite difference method in conjunction with Gauss–Seidel iterative technique. A computer code is prepared for the purpose. Exhaustive numerical studies are performed to elucidate the effects of parameters like volumetric heat generation, thermal conductivity, surface emissivity and convection heat transfer coefficient on local temperature distribution, peak device temperature and relative contributions of convection and radiation in heat dissipation.

Keywords Square-shaped electronic device · Discrete heat sources · Conduction · Convection · Radiation · Interaction

A. P. Shah · Y. M. Krishna · C. G. Rao (✉)
Department of Mechanical Engineering, National Institute of Technology, Warangal 506 004, Andhra Pradesh, India
e-mail: cgr_gcr@yahoo.co.in

List of symbols

h	Convection heat transfer coefficient (W/m^2 K)
k	Thermal conductivity of the material of the slab (W/m K)
L	Length of each side of the square shaped slab (m)
L_h	Length and height of each of the discrete heat sources in the slab (m)
M	Number of nodes along the X direction of the slab
$M_{1,2,3,4}$	Node numbers at the interface of non-heat source and heat source portions along X direction, respectively, from left to right boundary
N	Number of nodes along the Y direction of the slab
$N_{1,2,3,4}$	Node numbers at the interface of non-heat source and heat source portions along Y direction, respectively, from bottom to top boundary
q_v	Volumetric heat generation in each of the heat sources (W/m^3)
T	Temperature at any location in the computational domain (K or °C)
T_∞	Ambient air temperature (°C)
T_{max}	Peak device temperature (°C)
x, y	Horizontal and vertical distances, respectively (m)

Greek Symbols

ε	Surface emissivity of the slab
σ	Stefan-Boltzmann constant (5.6697×10^{-8} W/m^2 K^4)

Subscripts

$q_{cond,y,in}$	Conduction heat transfer into an element in Y direction
$q_{cond,y,out}$	Conduction heat transfer out of an element in Y direction

$q_{cond,x,in}$	Conduction heat transfer into an element in X direction
$q_{cond\ x,out}$	Conduction heat transfer out of an element in X direction
q_{conv}	Convection heat transfer from an element
q_{rad}	Radiation heat transfer from an element
i	Any arbitrary element along X direction
j	Any arbitrary element along Y direction

Introduction

Numerous analytical, numerical and experimental studies are available in the literature that address multi-mode heat transfer from different kinds of geometries with varying complexities. Zinnes [1] is one of those initial researchers, who presented the results of the problem of combined conduction and laminar convection from a vertical flat plate of finite thickness with an arbitrary heating distribution over its surface. Kim and Anand [2, 3] studied, numerically, the effect of wall conduction on free convection between asymmetrically heated vertical plates for the cases of uniform wall heat flux and uniform wall temperature, respectively. An experimental study on the fundamental aspects of conjugate mixed convection from two heat sources of finite width and negligible thickness having uniform heat flux input at the surface has been performed by Tewari and Jaluria [4]. Gorski and Plumb [5] numerically investigated the problem of conjugate laminar forced convection from a single discrete heat source that is flush mounted in a flat plate. Merkin and Pop [6] analyzed, numerically, the problem of conjugate free convection from a vertical surface, wherein they normalized the governing boundary-layer equations for fluid flow making use of only Prandtl number as the independent parameter. Hossain and Takhar [7] performed numerical studies on interaction of surface radiation with combined forced and free convection flow of a viscous incompressible fluid past a heated vertical plate for the twin cases of uniform free stream and uniform surface temperatures. Dehghan and Behnia [8] made a thorough study on combined natural convection, conduction and radiation from an open cavity provided with discrete heating along the left wall. Vynnycky and Kimura [9] investigated, both analytically and numerically, two-dimensional conjugate free convection from a vertical plate in communication with a semi-infinite fluid region. Watson et al. [10] conducted numerical study of laminar mixed convection between a series of vertically aligned parallel plates provided with planar heat sources. Cole [11] has presented his results of the problem of conjugate heat transfer from a small heated strip.

With regard to multi-mode heat transfer studies that incorporate mixed convection coupled with conduction and surface radiation, Gururaja Rao et al. [12] presented results of conjugate mixed convection with radiation from a vertical plate equipped with a discrete heat source. Here, they solved the problem without the conventional boundary layer approximations. Subsequently, the same authors [13] solved the conjugate heat transfer problems pertaining to the geometry of vertical channel, with respectively, uniform wall heat generation and discrete wall heat generation. Gururaja Rao [14] studied the effect of traversing the discrete heat source along a vertical electronic board subjected to buoyancy-aided mixed convection with conduction and radiation. Kanna and Das [15] provided an analytical solution for conjugate forced convection heat transfer from a flat plate exposed to a laminar jet flow making use of boundary layer theory. Gururaja Rao et al. [16] presented the results of their numerical probe into conjugate convection with radiation from an open cavity with a flush-mounted heat source. Sawant and Gururaja Rao [17] furnished the findings of their studies on conjugate mixed convection with surface radiation from a vertical electronic board with multiple discrete heat sources. The same authors [18] provided a numerical solution for the geometry of a uniformly heated vertical plate. Recently, Ganesh Kumar and Gururaja Rao [19, 20] solved the problem of conjugate mixed convection with surface radiation from a vertical plate with multiple non-identical heat sources.

A thorough literature review on multi-mode heat transfer, a brief summary of which has been provided above, reveals that the geometry of a square-shaped electronic device with multiple flush-mounted discrete heat sources has not been adequately explored. In view of this, the present paper takes up a detailed numerical investigation into conjugate convection with radiation from an electronic device modeled as a square slab equipped with four symmetrically spaced identical flush-mounted discrete heat sources.

Problem Definition and Mathematical Formulation

Figure 1 shows the problem geometry considered in the presented study. It consists of a square-shaped slab of each side of length L. There are four identical embedded discrete heat sources of dimensions $L_h \times L_h$ in this slab, which are located symmetrically at the geometric centers of the four quadrants of the square slab. There is a uniform volumetric heat generation at the rate q_v W/m^3 in each heat source. The thermal conductivity and surface emissivity of the square slab are, respectively, k and ε.

The heat generated in all heat sources is initially conducted along and across the electronic board, before getting dissipated from the boundaries of the device by combined convection and radiation. The cooling medium is air at

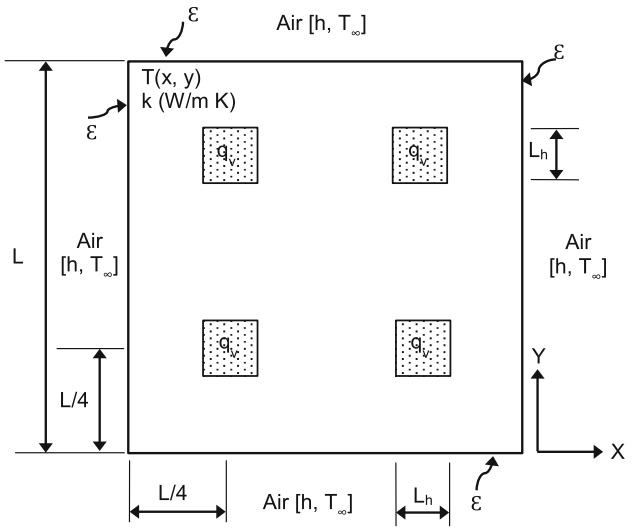

Fig. 1 The problem geometry considered for study along with system of co-ordinates

temperature T_∞, while the convection heat transfer coefficient is h W/m^2 K. Further, air is considered to be transparent to thermal radiation. The governing equations for temperature distribution in the entire computational domain are obtained by making energy balance between the heat generated, conducted, convected and radiated. For example, the governing equation for all the interior nodes of each of the four discrete heat sources, upon energy balance, turns out to be:

$$\frac{\partial^2 T}{\partial x^2}+\frac{\partial^2 T}{\partial y^2}+\frac{q_v}{k}=0 \tag{1}$$

With regard to interior nodes in non-heat source portions, the governing equation would be Eq. (1) with source term absent.

$$\frac{\partial^2 T}{\partial x^2}+\frac{\partial^2 T}{\partial y^2}=0 \tag{2}$$

For a typical interface element between the left boundary of the left top heat source and the non-heat source portion, the energy balance turns out to be:

$$q_{cond,x,in}+q_{cond,y,in}+q_v\left(\frac{y_{j+1}-y_{j-1}}{2}\right)\left(\frac{x_{i+1}-x_{i-1}}{2}\right) = q_{cond,x,out}+q_{cond,y,out} \tag{3}$$

Substituting various terms in the above equation and simplifying, one gets:

$$\frac{\partial^2 T}{\partial x^2}+\frac{\partial^2 T}{\partial y^2}+\frac{q_v}{k}\left(\frac{x_{i+1}-x_i}{x_{i+1}-x_{i-1}}\right)=0 \tag{4}$$

With regard to the boundaries of the board, making energy balance on an arbitrarily chosen semi-element along the left boundary:

$$q_{cond,y,in}=q_{cond,x,out}+q_{cond,y,out}+q_{conv}+q_{rad} \tag{5}$$

Substitution of appropriate expressions for various terms in the above equation and subsequent simplification leads to the following governing equation for temperature distribution along the left boundary of the board:

$$\frac{\partial^2 T}{\partial y^2}\left(\frac{x_2-x_1}{2}\right)+\frac{\partial T}{\partial x}+\frac{h}{k}(T_\infty-T)+\frac{\sigma\varepsilon}{k}\left(T_\infty^4-T^4\right)=0 \tag{6}$$

With regard to the corner elements, for a typical top corner element of the right boundary, the governing equation for temperature distribution would get modified as:

$$\frac{\partial T}{\partial x}\left(\frac{y_n-y_{n-1}}{2}\right)+\frac{\partial T}{\partial y}\left(\frac{x_m-x_{m-1}}{2}\right)+\left(\frac{h}{k}(T-T_\infty)+\frac{\sigma\varepsilon}{k}\left(T^4-T_\infty^4\right)\right)\times\left(\frac{y_n-y_{n-1}}{2}+\frac{x_m-x_{m-1}}{2}\right)=0 \tag{7}$$

The governing equations for temperature distribution pertaining to the rest of the elements of the computational domain are also obtained using similar treatment as above.

Solution Methodology

The governing equations for temperature distribution in the entire computational domain obtained as above are the partial differential equations. These equations are transformed into algebraic equations through finite volume method. For example, Eq. (1), after being transformed into algebraic form, yields the following expression for the temperature at any interior node of each of the four discrete heat source portions.

$$T_p=\frac{T_{i+1,j}A_E+T_{i-1,j}A_W+T_{i,j+1}A_N+T_{i,j-1}A_S+\frac{q_v}{2k}(x_{i+1}-x_{i-1})(y_{j+1}-y_{j-1})}{A_E+A_W+A_N+A_S} \tag{8}$$

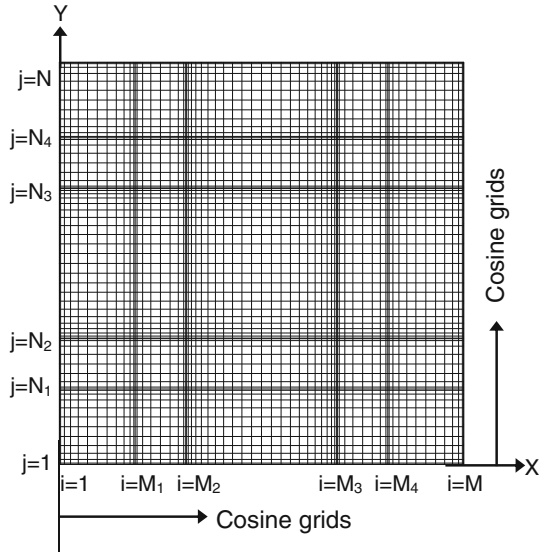

Fig. 2 Grid system used for discretization of the computational domain

where A_E, A_W, A_N and A_S are the non-dimensional geometric parameters defined as:

$$A_E = \frac{y_{j+1} - y_{j-1}}{x_{i+1} - x_i}; A_W = \frac{y_{j+1} - y_{j-1}}{x_i - x_{i-1}}; A_N = \frac{x_{i+1} - x_{i-1}}{y_{j+1} - y_j};$$
$$A_S = \frac{x_{i+1} - x_{i-1}}{y_j - y_{j-1}} \quad (9)$$

The expression for the temperature at any interior node of the non-heat source portions of the square slab turns out to be identical to Eq. (8) with source term absent. A similar approach is adopted for the rest of the computational domain. The algebraic equations thus obtained are solved simultaneously using Gauss–Seidel iterative solver. It is to be noted that, as can be clearly seen from Fig. 2, an unequi-spaced grid system is used for the discretization of the computational domain. In particular, a cosine function is employed such that the grids are always finer nearer to the boundaries, while they get coarser in between.

Full relaxation has been employed on temperature during the iterations, while for terminating the iterations, a convergence criterion of 10^{-8} has been used. A computer code in C^{++} is written to solve the problem.

Ranges of Parameters

Results are obtained for a square slab of dimensions, L × L = 20 cm × 20 cm, while each of the four discrete heat sources is taken to be of size, $L_h \times L_h$ = 2.5 cm × 2.5 cm. The volumetric heat generation (q_v) is taken to be generally equal to 10^5 W/m^3, though the code written is found to be working with other values of q_v as well. With regard to grid system, 161 × 161 unequi-spaced grids, generated in the manner described elsewhere, are used, while each heater is discretized considering 21 × 21 grids. Air is taken to be the cooling agent and is assumed to be radiatively transparent at a temperature (T_∞) of 25 °C. The thermal conductivity (k) of the slab as well as heat sources is varied between 0.25 and 1 W/m K. This is done keeping in mind the fact that the materials typically used for electronic devices have thermal conductivity of the order of unity. The convection heat transfer coefficient (h) is varied between 5 and 100 W/m^2 K. Here, the value of h for the asymptotic free convection limit is taken to be 5 W/m^2 K, while that for the asymptotic forced convection limit is 100 W/m^2 K. With regard to surface emissivity (ε) of the slab, generally the range of 0.05–0.85 is chosen. Here, ε = 0.05 pertains to a good reflector (like highly polished aluminum) and ε = 0.85 refers to a good emitter (like black paint). In addition to the above range that is typically used, while bringing out the exclusive effect of radiation, ε = 0 and ε = 1 too are chosen to address the two diametrically opposite cases of (i) radiation not taken into account and (ii) radiation taken into reckoning.

Results and Discussion

Variation of Local Temperature of the Device with Other Parameters

One of the prime concerns a heat transfer engineer faces in electronic cooling applications is to keep the temperature distribution in the device in control under varying operating conditions. Keeping the above in mind, Fig. 3 is plotted to study the nature of the variation of the local temperature distribution for different values of surface emissivity (ε) and for a given fixed input of the rest of the parameters. In particular, the figure pertains to the temperature distribution in the horizontal direction at y = L/4. It can be seen that all the three local temperature profiles exhibit similar pattern. For a given surface emissivity (ε), the temperature is increasing sharply as one moves away from the left boundary of the device, reaching a first local maximum at the center of the left bottom heat source. It is again decreasing progressively as one goes through the non-heat source portion between the two heat sources. After reaching a local minimum, the temperature again increases and a similar behavior as noticed along the first heat source is observed along the second heat source portion as well. The second local maximum temperature is equal to the first local maximum and is incidentally the maximum temperature of the device. The observation of the two local maximums in the two heat source portions of the device is due to the occurrence of bulk heat transfer activity in those regions. The figure further shows that the temperature at any location along the device decreases as surface

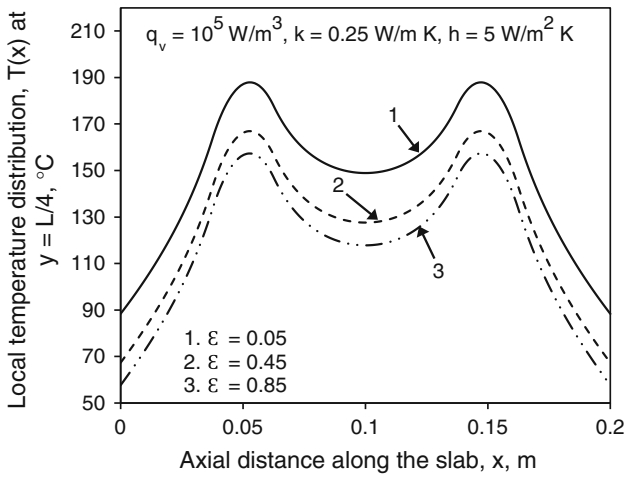

Fig. 3 Local temperature profiles for various surface emissivities of the slab

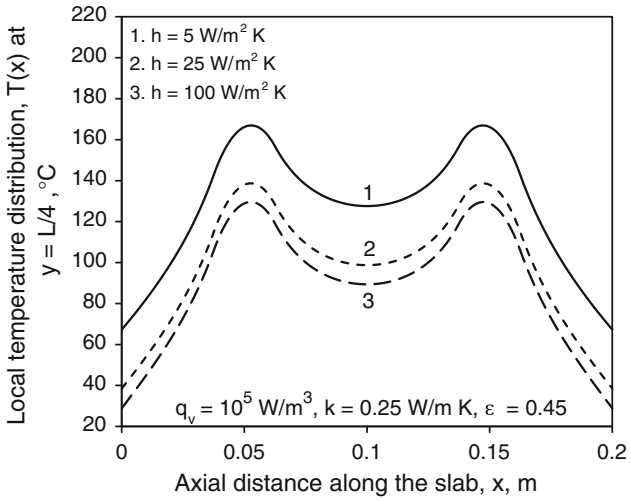

Fig. 4 Local temperature profiles in various regimes of convection

emissivity increases, owing to increased radiative heat dissipation from the device. In the present example, at x = L/4, the temperature decreases by 11.19 % as ε increases from 0.05 to 0.45, while the drop in temperature is by 5.77 % with subsequent increase in ε to 0.85.

Figure 4 describes the nature of variation of local temperature in the horizontal direction at the same location in vertical direction as in Fig. 3 in different regimes of convection. Again here, a fixed input of q_v, k and ε is chosen, as shown. The trend followed by the temperature profile for a given h, looks similar to what has been noticed in Fig. 3. Like in the earlier case, for each of the three curves, there are two identical local maximum temperatures, being the maximum temperature of the device. The figure reveals that, the temperature at any location along the device decreases as flow transits from free convection to forced convection dominant regime. This is in view of increased convection activity from the surface of the slab owing to increased convection heat transfer coefficient (h). For example, the first local maximum temperature is dropping by 17.1 % with change in h from 5 to 25 W/m^2 K and the same is dropping by 6.65 % with further increase in h from 25 to 100 W/m^2 K. The figure thus explains the role of impressed velocity (u_∞) in influencing the slab temperature for the given values of thermal conductivity of the material of the device and surface emissivity (k and ε, respectively).

In order to probe into the effect of the thermal conductivity (k) of the material of the device on the local temperature distribution, a study is performed considering three different values of k, viz. 0.25, 0.5 and 1 W/m K (Fig. 5). It is to be noted here that the above values of k are chosen to address the typically used material for electronic boards. Further, the present study pertains to a fixed set of other parameters (q_v, h and ε) as shown. As can be seen, the general trend of the temperature profile is again the same as in Figs. 3 and 4. The local temperature at any location in the device comes down with increasing k on account of increased percolation of heat along the board. In the present example, the second local maximum temperature at the center of the right bottom heat source portion decreases by 53.21 % as k increases from 0.25 to 1 W/m K. However, the temperature profile gets progressively flatter with increasing thermal conductivity of the device as shown. This means, towards larger values of k, there is hardly any temperature gradient noticed along the device and the device almost appears to be isothermal.

Variation of Maximum Device Temperature with Other Parameters

In addition to having the knowledge of temperature distribution in the entire slab, the heat transfer engineer dealing with cooling system design would be primarily concerned with control of the peak temperature (T_{max}) assumed by the device over a wide range of operating conditions.

Figure 6 depicts the dependence of T_{max} on surface emissivity (ε) of the electronic device in different regimes of convection. The four convection heat transfer coefficients chosen are h = 5, 10, 25 and 100 W/m^2 K. Here, h = 5 W/m^2 K is considered to be the asymptotic limit of free convection, while h = 100 W/m^2 K is taken to be the asymptotic forced convection limit. Five different values of ε, namely 0.05, 0.25, 0.45, 0.65 and 0.85, are tried by keeping the remaining input parameters, viz. $q_v = 10^5$ W/m^3 and k = 0.25 W/m K, fixed. It can be seen from the figure that, in all regimes of convection, T_{max} decreases

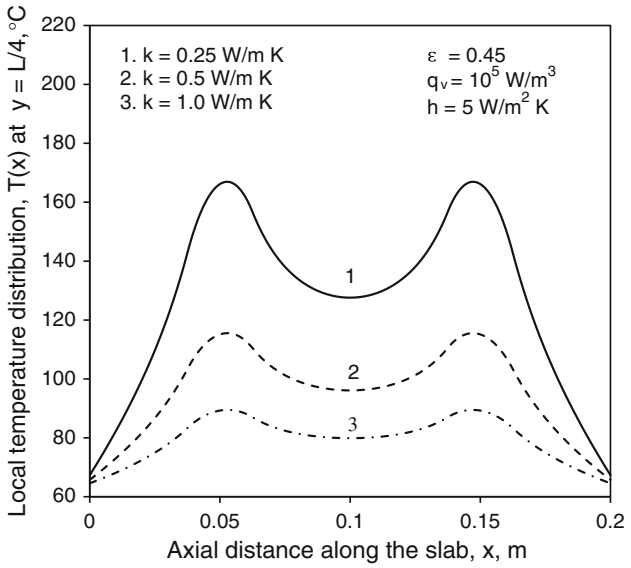

Fig. 5 Local temperature profiles for various thermal conductivities of the slab material

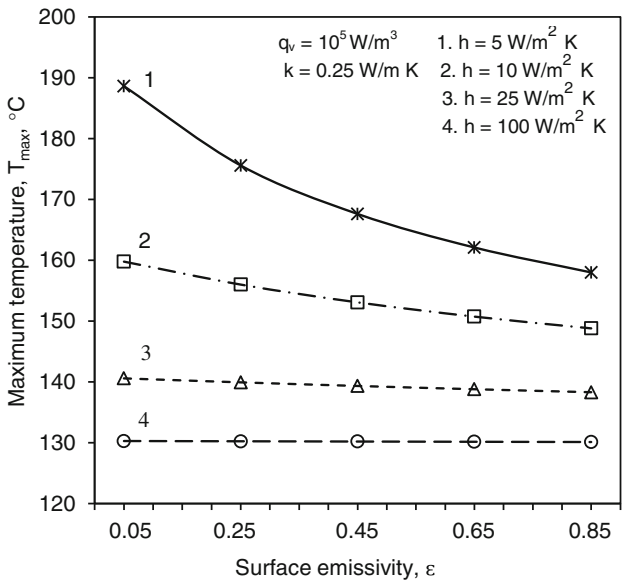

Fig. 6 Variation of maximum temperature of the square slab with surface emissivity in different regimes of convection

with increasing ε on account of increased share from radiation in dissipating the heat from the device. However, the effect of ε is distinctly noticed for smaller values of h (<25 W/m^2 K). This is because, in the regime of convection pertaining to the above range, convection is predominantly out of buoyancy and thus is only to a smaller extent, which enables radiation to dominate in surface heat dissipation. In contrary to the above, with larger values of h taken, forced convection creeps in and thus one can see a notional drop in T_{max} with increasing ε (see curves 3 and 4). The figure also implicitly shows that, for a given ε, one can control the maximum device temperature by expending more pumping power and thus operating with increased values of h. To quantify the observations made above, in the present study, T_{max} drops down by 16.24 % with ε increasing from 0.05 to 0.85 for h = 5 W/m^2 K. On the other hand, for h = 100 W/m^2 K, T_{max} comes down by a mere 0.13 % as a result of the same increment in ε. Further, for ε = 0.05, a drop of 30.94 % in T_{max} is observed by changing the h from 5 to 100 W/m^2 K. This study demonstrates the relevance of surface emissivity in influencing maximum device temperature in all regimes of convection, especially in the cases of free convection.

The interaction between internal conduction of heat in the slab and the convection heat transfer coefficient (h) in influencing the maximum device temperature (T_{max}) is narrated in Fig. 7. The study is performed by considering six different values of h and three typical values of k, as depicted in the figure. The results are obtained for constant values of $q_v = 10^5$ W/m^3 and ε = 0.45. For a given k, T_{max} is decreasing with increase in h, while the decrease in T_{max} is less pronounced towards larger values of h in comparison to that for the smaller values of h. In the present example, for k = 0.25 W/m K, T_{max} is dropping down by 16.87 % as h increases from 5 to 25 W/m^2 K, while with subsequent increase of h to 100 W/m^2 K, T_{max} is decreasing by just 6.5 %. This conveys the message that not much cooling is accomplished despite increasing the pumping power expended and thus the electric power consumed beyond, say h = 25 W/m^2 K. Thus, it could be taken as a tacit optimum value for h. Figure further makes it clear that, with increase in k, one can observe a marked drop in T_{max} in all regimes of convection. For example, for

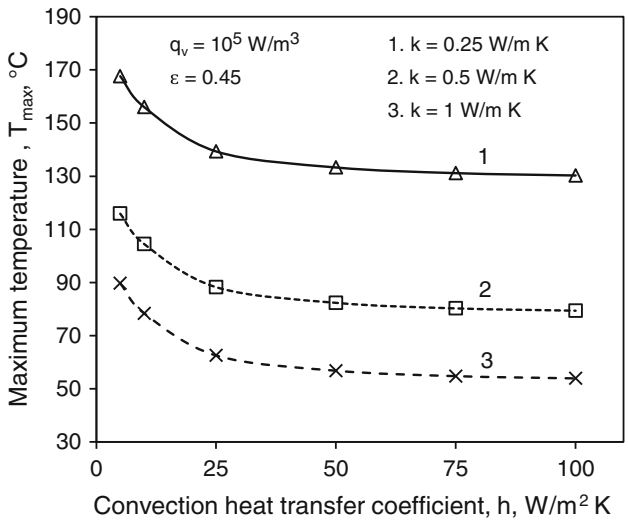

Fig. 7 Variation of maximum temperature of the square slab with convection heat transfer coefficient for different values of thermal conductivity

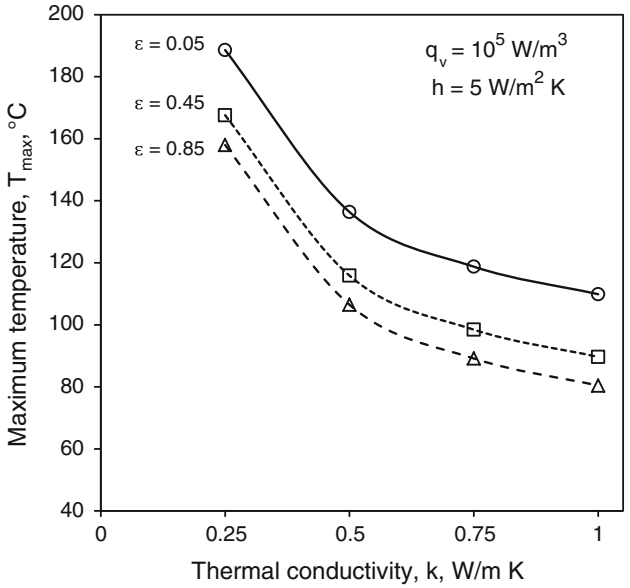

Fig. 8 Variation of maximum temperature of the square slab with thermal conductivity for three typical surface emissivity values

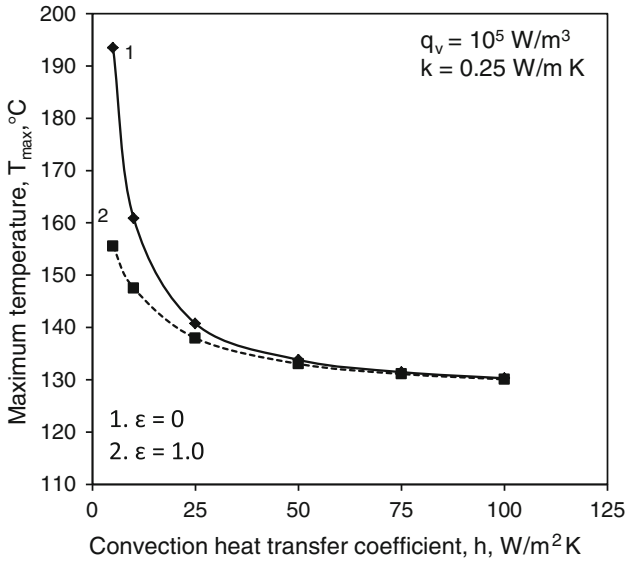

Fig. 9 Peak slab temperature in various regimes of convection demonstrating the exclusive effect of surface radiation

h = 5 W/m^2 K, with increase in k from 0.25 to 1 W/m K, T_{max} is coming down by 46.5 %.

A study on variation of T_{max} with thermal conductivity (k) of the slab material for three typical values of emissivity (ε) has been performed holding q_v and h fixed. The results of the above study are represented in Fig. 8. Figure shows that, for a given surface emissivity, T_{max} decreases with increasing k on account of increase in diffusion of heat through the slab. Though the trend continues with all values of k, the rate of drop in T_{max} diminishes towards larger values of k. Further, for a given thermal conductivity, the figure shows a considerable drop in T_{max} with increase in surface emissivity. As an example, for ε = 0.05, an increase in k from 0.25 to 0.5 W/m K results in a remarkable drop of 27.7 % in T_{max}. A subsequent increase in k to 0.75 and 1 W/m K, respectively, brings down T_{max} by 12.9 % and 7.4 %. Further, in the present case, for k = 0.25 W/m K, T_{max} is dropping down by 16.24 % as ε rises from 0.05 to 0.85.

Exclusive Effect of Surface Radiation

Since the prime objective of the present study has been to underline the significance of contribution from radiation in problems of this kind that make use of gaseous cooling media (air), a study is performed to exclusively bring out the role of ε in controlling T_{max} over the entire convection regime.

Figure 9 shows the variation of maximum board temperature (T_{max}) with convection heat transfer coefficient for two limiting values of surface emissivity (ε), namely (i) ε = 0 (radiation absent) and (ii) ε = 1 (best possible radiation). The results are obtained for the fixed input of $q_v = 10^5$ W/m^3 and k = 0.25 W/m K. It can be seen that radiation, when ignored in calculations, leads to overestimation of peak device temperature in all regimes of convection, in general, and in free convection dominant regime, in particular. In the current study, consideration of radiation (that too with the best possible emissivity) is bringing down the peak device temperature by as much as 19.61 % for h = 5 W/m^2 K, whereas for h = 100 W/m^2 K, the drop is meager and is by 0.16 %.

Relative Contributions of Convection and Radiation in Heat Dissipation From the Device

Since the heat generated in the four embedded discrete heat sources in the device is dissipated from its boundaries by combined modes of convection and radiation, a study of the roles played by the above two mechanisms is mandatory. In view of the above, Fig. 10 is plotted depicting the results of a study made for the fixed input of q_v and k shown there in. Three typical limiting values for h have been chosen. The asymptotic free convection limit pertains to h = 5 W/m^2 K, while the asymptotic forced convection limit is represented by h = 100 W/m^2 K. With regard to surface emissivity (ε), five different values are selected from 0.05 to 0.85. As already mentioned, the lower and the upper limits of ε pertain to good reflector and good emitter, respectively.

The figure indicates that, in a given regime of convection, the contribution to heat dissipation by convection progressively decreases as ε increases from 0.05 to 0.85, with the contribution from radiation showing a mirror image

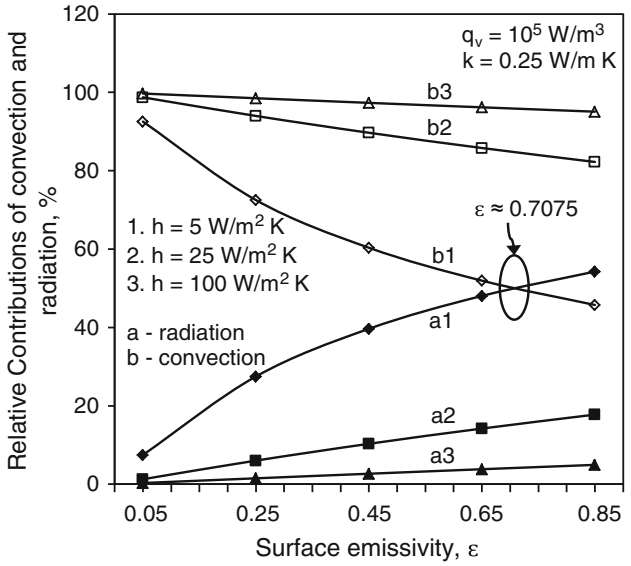

Fig. 10 Relative contributions of convection and radiation with surface emissivity in different convection regimes

increase. However, for h = 100 W/m^2 K that indicates forced convection dominance, there is an expected lead role taken by convection, with radiation showing a limited effect. When once the flow regime transits to free convection (h = 5 W/m^2 K), radiation starts showing an improved effect on heat dissipation from the slab. This point is substantiated from the curve (a1) of the above figure, which pertains to h = 5 W/m^2 K. Here, the contribution of radiation increases from 7.46 to 54.26 % as one changes the surface coating of the slab from a good reflector (ε = 0.05) to a good emitter (ε = 0.85). This study underlines the importance of radiation in problems of this class, specifically if one is working in the regime of free convection. Further, the two curves belonging to convection and radiation for h = 5 W/m^2 K cross each other at ε ≈ 0.7075, where convection and radiation take an identical share in heat dissipation with radiation overriding convection thereafter. Though not as pronounced as above, a similar trend is observed in the roles played by convection and radiation even towards larger values of h. These results caution the designer not to overlook radiation in any of the regimes of convection due to the fact that it contributes about 5 % to heat dissipation even for h = 100 W/m^2 K (forced convection dominant regime) when ε = 0.85.

Study of Isotherm Patterns in the Device

Figure 11 shows the isotherm plots within the slab drawn for a typical input ($q_v = 10^5$ W/m^3, k = 0.25 W/m K and h = 5 W/m^2 K) and for three different values of ε, viz. 0.05, 0.45 and 0.85. It can be seen that, for a given ε, there is a well-defined symmetry in the isotherms with major heat transfer activity noticed at the four discrete heat source portions of the slab. There are four identical peaks noticed at the geometric centers of the four heat sources. With heat percolating from the heat sources through the rest of the slab towards the boundaries, there is an expected decrement in the local temperature in all the directions from each of the heat sources. Though the nature of isotherms is similar for all the three values of ε chosen, one can clearly see a progressive decrease in the temperatures pertaining to the isotherms with increasing ε. This clearly underlines the effect radiation shows in deciding the nature of temperature distribution in the slab. Further the above decrement in temperature is observed to be more pronounced between ε = 0.05 and 0.45 (Fig. 11a, b) when compared to that between ε = 0.45 to 0.85.

In order to study the nature of isotherms within the slab in different regimes of convection, a family of three contour plots is drawn for h = 5, 25 and 100 W/m^2 K, as shown in Fig. 12. The entire study made here is for the fixed input, comprising $q_v = 10^5$ W/m^3, ε = 0.05 and k = 0.25 W/m K. The figure clearly shows that, as in the case of Fig. 11, here too, for a given h, symmetry in isotherms is clearly observed with major heat transfer activity occurring at the four discrete heat sources. The temperature is identical at the geometric centers of all the heat sources, which, incidentally, is the maximum device temperature too. The nature of isotherms is similar in all regimes of convection. However, with increase in h, the temperatures related to isotherms decrease owing to increased convection heat dissipation. The above effect of convection heat transfer coefficient is significant between 5 and 25 W/m^2 K (Fig. 12a, b), while it peters down as its value increases further from 25 to 100 W/m^2 K (Fig. 12b, c).

Figure 13 describes the effect of internal conduction on isotherm patterns for constant values of $q_v = 10^5$ W/m^3, ε = 0.05 and h = 5 W/m^2 K and for three typical values of k, namely 0.25, 0.5 and 1 W/m K. The figure clearly depicts the symmetry in isotherms for all values of k chosen as has been noticed in the above two cases, viz. (i) variable ε and (ii) variable h. There is a progressive decrease in the temperature of isotherms with increase in k. However, the above effect of k on temperature is more pronounced in the vicinity of all discrete heat sources. Further, for smaller values of k, one can observe the crowding of isotherms in comparison to that with larger values of the same. This, in turn, represents steeper temperature gradients within the slab due to poorer percolation of heat from the heat sources through the slab towards the boundaries. This clearly helps one to control the temperature distribution within the slab, and thus the peak device temperature, by selecting a proper material for the slab.

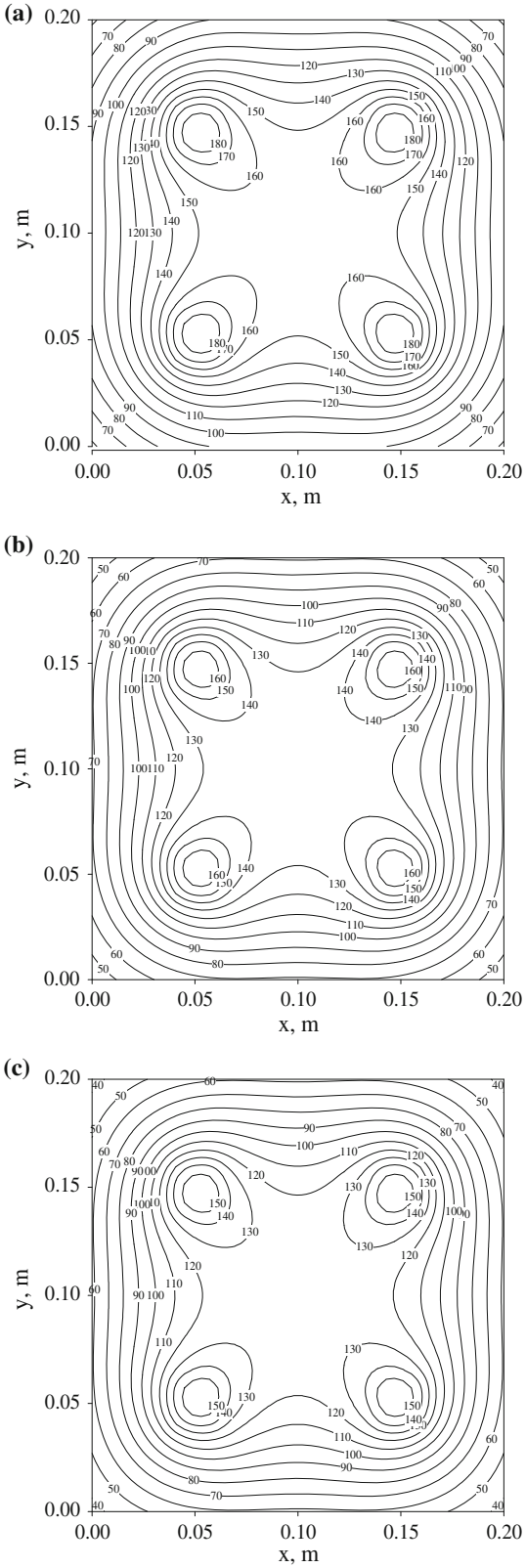

Fig. 11 Isotherm plots in the slab in °C for different surface emissivities. **a** $\varepsilon = 0.05$, **b** $\varepsilon = 0.45$, **c** $\varepsilon = 0.85$

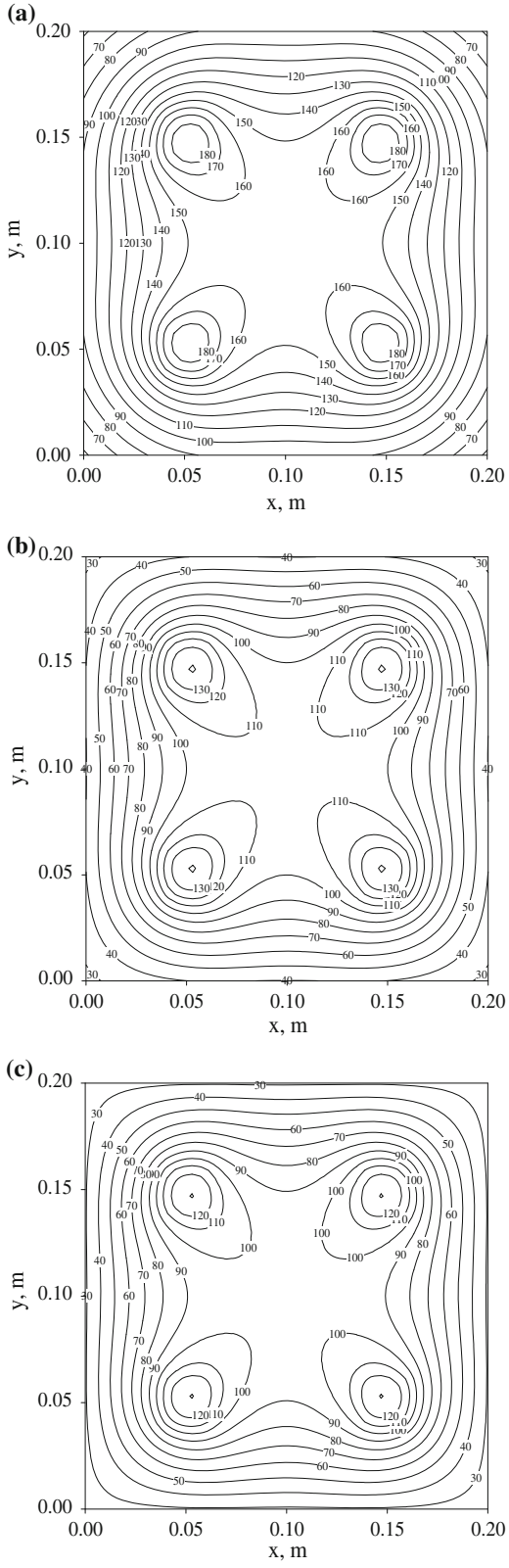

Fig. 12 Isotherm plots in the slab in °C in different regimes of convection. **a** h = 5 W/m^2 K, **b** h = 25 W/m^2 K, **c** h = 100 W/m^2 K

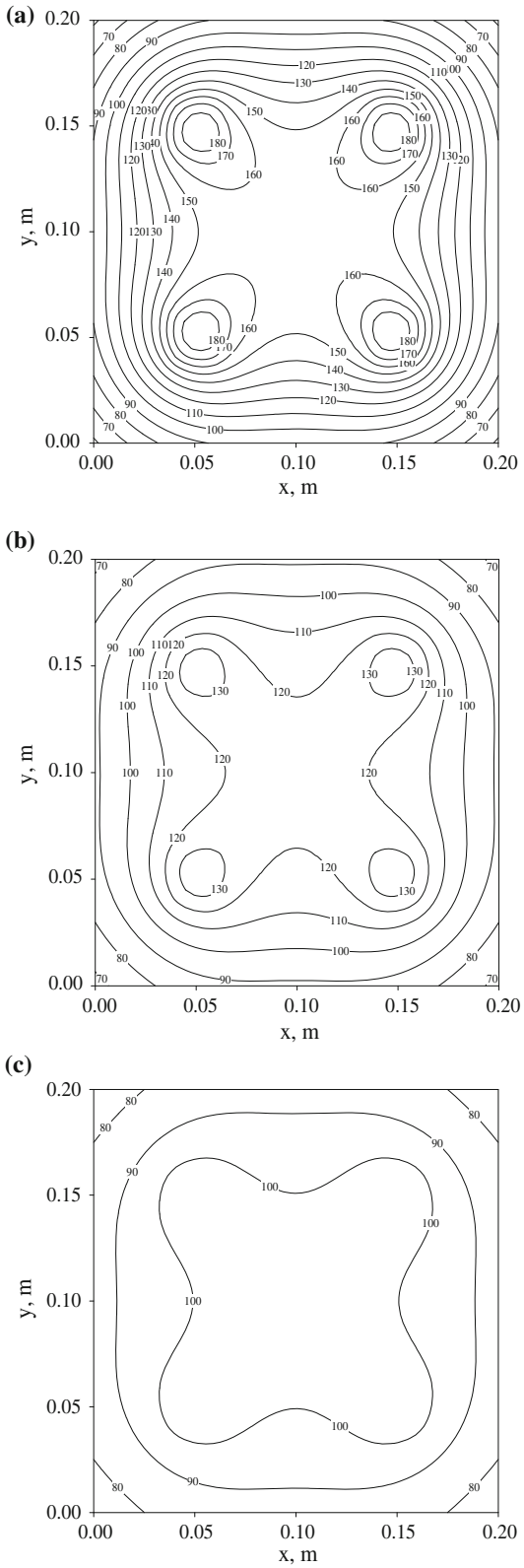

Fig. 13 Isotherm plots in the slab in °C for different values of thermal conductivity. **a** k = 0.25 W/m K, **b** k = 0.5 W/m K, **c** k = 1 W/m K

Concluding Remarks

The problem of conjugate convection with surface radiation from a square-shaped electronic device embedded with four symmetrically located flush-mounted discrete heat sources has been numerically solved. A computer code in C^{++} has been written for the above job. A number of parametric studies have been performed to bring out the roles of thermal conductivity, convection heat transfer coefficient and surface emissivity in influencing various results concerning the problem. The results considered included the local temperature distribution, the peak device temperature, the relative contributions of convection and radiation and the isotherm contour plots in the device.

In addition to the above, attempts are made to extract the effect of surface radiation by solving the problem (i) without radiation and (ii) with radiation considering the highest possible emissivity. The gross error that creeps in on ignoring radiation has been highlighted in all the regimes of convection. It is further noticed that radiation could even override convection in heat dissipation from the device while operating in free convection dominant regime.

References

1. A.E. Zinnes, The coupling of conduction with laminar natural convection from a vertical flat plate with arbitrary surface heating. ASME J. Heat Transf. **92**, 528–534 (1970)
2. S.H. Kim, N.K. Anand, W. Aung, Effect of wall conduction on free convection between asymmetrically heated vertical plates: uniform wall heat flux. Int. J. Heat Mass Transf. **33**, 1013–1023 (1990)
3. N.K. Anand, S.H. Kim, W. Aung, Effect of wall conduction on free convection between asymmetrically heated vertical plates: uniform wall temperature. Int. J. Heat Mass Transf. **33**, 1025–1028 (1990)
4. S.S. Tewari, Y. Jaluria, Mixed convection heat transfer from thermal sources mounted on horizontal and vertical surfaces. ASME J. Heat Transf. **112**, 975–987 (1990)
5. M.A. Gorski, O.A. Plumb, Conjugate heat transfer from an isolated heat source in a plane wall, in *Proceedings of winter annual meeting of the American society of mechanical engineers*, ASME HTD, vol. 210, pp. 99–105 (1992)
6. J.H. Merkin, I. Pop, Conjugate free convection on a vertical surface. Int. J. Heat Mass Transf. **39**, 1527–1534 (1996)
7. M.A. Hossain, H.S. Takhar, Radiation effect on mixed convection along a vertical plate with uniform surface temperature. Int. J. Heat Mass Transf./Waerme-und Stoffuebertragung **31**, 243–248 (1996)
8. A.A. Dehghan, M. Behnia, Combined natural convection-conduction and radiation heat transfer in a discretely heated open cavity. ASME J. Heat Transf. **118**, 56–64 (1996)
9. M. Vynnycky, S. Kimura, Conjugate free convection due to heated vertical plate. Int. J. Heat Mass Transf. **39**, 1067–1080 (1996)

10. J.C. Watson, N.K. Anand, L.S. Fletcher, Mixed convective heat transfer between a series of vertical parallel plates with planar heat sources. ASME J. Heat Transf. **118**, 984–990 (1996)
11. K.D. Cole, Conjugate heat transfer from a small heated strip. Int. J. Heat Mass Transf. **40**, 2709–2719 (1997)
12. C. Gururaja Rao, C. Balaji, S.P. Venkateshan, Conjugate mixed convection with surface radiation from a vertical plate with discrete heat source. ASME J. Heat Transf. **123**, 698–702 (2001)
13. C. Gururaja Rao, C. Balaji, S.P. Venkateshan, Effect of surface radiation on conjugate mixed convection in a vertical channel with a discrete heat source in each wall. Int. J. Heat Mass Transf. **45**, 3331–3347 (2002)
14. C. Gururaja Rao, Buoyancy-aided mixed convection with conduction and surface radiation from a vertical electronic board with a traversable discrete heat source. Numer. Heat Transf. A **45**, 935–956 (2004)
15. P.R. Kanna, M.K. Das, Conjugate forced convection heat transfer from a flat plate by laminar plane wall jet flow. Int. J. Heat Mass Transf. **48**, 2896–2910 (2005)
16. C. Gururaja Rao, V. Nagabhushana Rao, C. Krishna Das, Simulation studies on multi-mode heat transfer from an open cavity with a flush-mounted discrete heat source. Heat Mass Transf. **44**, 727–737 (2008)
17. S.M. Sawant, C. Gururaja Rao, Conjugate mixed convection with surface radiation from a vertical electronic board with multiple discrete heat sources. Heat Mass Transf. **44**, 1485–1495 (2008)
18. S.M. Sawant, C. Gururaja Rao, Combined conduction-mixed convection-surface radiation from a uniformly heated vertical plate. Chem. Eng. Commun. **197**(6), 881–899 (2010)
19. G. Ganesh Kumar, C. Gururaja Rao, Interaction of surface radiation with conjugate mixed convection from a vertical plate with multiple non-identical discrete heat sources. Chem. Eng. Commun. **198**(5), 692–710 (2011)
20. G. Ganesh Kumar, C. Gururaja Rao, Parametric studies and correlations for combined conduction-mixed convection-radiation from a non-identically and discretely heated vertical plate. Heat Mass Transf. **48**, 505–517 (2011)